

Article

Investigation of the Deactivation Phenomena Occurring in the Cyclohexane Photocatalytic Oxidative Dehydrogenation on $\text{MoO}_x/\text{TiO}_2$ through Gas Phase and *in situ* DRIFTS Analyses

Vincenzo Vaiano ¹, Diana Sannino ^{1,*}, Ana Rita Almeida ², Guido Mul ² and Paolo Ciambelli ¹

¹ Department of Industrial Engineering, University of Salerno, Via Giovanni Paolo II, 132; 84084, Fisciano, SA, Italy; E-Mails: vvaiano@unisa.it (V.V.); pciambelli@unisa.it (P.C.)

² Faculty of Science & Technology, University of Twente, PO Box 217, Meander 225, 7500 AE, Enschede, The Netherlands; E-Mails: A.R.Almeida@tudelft.nl (A.R.A.); G.Mul@tudelft.nl (G.M.)

* Author to whom correspondence should be addressed; E-Mail: dsannino@unisa.it; Tel.: +39-8996-4092; Fax: +39-8996-4057.

Received: 16 August 2013; in revised form: 13 September 2013 / Accepted: 10 December 2013 /

Published: 13 December 2013

Abstract: In this work, the results of gas phase cyclohexane photocatalytic oxidative dehydrogenation on $\text{MoO}_x/\text{SO}_4/\text{TiO}_2$ catalysts with DRIFTS analysis are presented. Analysis of products in the gas-phase discharge of a fixed bed photoreactor was coupled with *in situ* monitoring of the photocatalyst surface during irradiation with an IR probe. An interaction between cyclohexane and surface sulfates was found by DRIFTS analysis in the absence of UV irradiation, showing evidence of the formation of an organo-sulfur compound. In particular, in the absence of irradiation, sulfate species initiate a redox reaction through hydrogen abstraction of cyclohexane and formation of sulfate (IV) species. In previous studies, it was concluded that reduction of the sulfate (IV) species via hydrogen abstraction during UV irradiation may produce gas phase SO_2 and thereby loss of surface sulfur species. Gas phase analysis showed that the presence of MoO_x species, at same sulfate loading, changes the selectivity of the photoreaction, promoting the formation of benzene. The amount of surface sulfate influenced benzene yield, which decreases when the sulfate coverage is lower. During irradiation, a strong deactivation was observed due to the poisoning of the surface by carbon deposits strongly adsorbed on catalyst surface.

Keywords: cyclohexane; gas phase analysis; DRIFTS analysis; deactivation

1. Introduction

Photocatalytic oxidation reactions have been widely used in processes such as the decontamination of water and air [1–8]. However, applications of heterogeneous photocatalysis for the synthesis of compounds of commercial importance have been considered only in recent years. The most studied photocatalytic reactions occur in slurry systems. Among them, partial oxidation of cyclohexane is an important commercial reaction, as the resultant products, cyclohexanol and cyclohexanone, are precursors in the syntheses synthesis of adipic acid, in turn intermediates in the production of nylon [9]. In their review, Maldotti *et al.* [10] reported the main aspects concerning the photocatalytic oxidation of cyclohexane. Li *et al.* [11] showed that the quantum size and surface state are key factors governing the selectivity in photooxidation on TiO₂ nanoparticles [12,13]. The photo-oxidation of cyclohexane on titanium dioxide was also investigated in neat cyclohexane and in various solvents showing an influence of the solvent media on the cyclohexane oxidation rate and on the selectivity to cyclohexanol and cyclohexanone [14,15].

From theoretical and practical points of view, the ideal solvent for the photo-oxidation of cyclohexane is one that minimizes the strengths of adsorption of the desired products on titanium dioxide and does not compete with cyclohexane and oxygen for adsorption sites. Otherwise, the solvent could be strongly adsorbed but is non-reactive with itself upon forming a radical on the illuminated titanium dioxide surface [16].

Supported transition-metal oxides can absorb light, and the transferred energy can be used to activate C-H bonds in saturated hydrocarbons, a chemical step that is generally unselective [6]. In this context, cyclohexanol, cyclohexanone, and polyoxygenates have been formed from cyclohexane when polyvanadate or polyoxytungstate were supported on several oxides [17,18].

It was shown that attenuated total reflection Fourier transform infrared (ATR-FTIR) is a suitable way to monitor in real time and *in situ* the light-induced heterogeneous oxidations [19], allowing deeper knowledge of the complex phenomena occurring under irradiation to be obtained. ATR-FTIR technique was also performed to study the photodegradation of organic pollutants in water on TiO₂ [20].

The generally low efficiency associated with liquid phase photocatalytic reactions, which typically occur at low conversion, coupled with the difficulty of separating catalyst and products in a liquid has motivated research of gas-solid systems, e.g., catalysts active in the gas-phase partial oxidation of cyclohexane. However, selective photooxidation of cyclohexane yields different reaction products in gas phase relative to liquid phase. In particular, cyclohexene or benzene are selectively obtained through gas phase oxidative dehydrogenation of cyclohexane on MoO_x/TiO₂ photocatalysts, with UV illumination both in fixed [21] and fluidized bed reactors [22–24]. Higher molybdenum loadings improved the benzene selectivity, whereas with only titania, total conversion to carbon dioxide is obtained. The selective formation of benzene is attributed to the poisoning by Mo-species of unselective sites on the titania surface which otherwise totally oxidize cyclohexane to CO₂ and water [24–26].

A mechanism for the catalytic photo-oxidative dehydrogenation of cyclohexane to benzene on MoO_x/TiO₂ was recently proposed by analyzing the gas-phase coming from a photoreactor [21]. This mechanism involves dehydrogenation of cyclohexane to cyclohexene followed by oxy-dehydrogenation to benzene on molybdenum oxide active sites via a detailed sequence of elementary steps [21]. In the

same paper, several hypotheses relating to the role of sulfate species in promoting the selectivity to benzene formation were postulated: (1) sulfate present on TiO₂ surface may facilitate hydrogen abstraction from an adsorbed cyclohexane molecule, owing to its strong acid properties, or (2) it may participate in the re-oxidation step of the octahedrally-coordinated polymolybdate surface species [21]. With regard to the influence of sulfate concentration, Ciambelli *et al.* [24,26,27] showed that during photooxidative dehydrogenation of cyclohexane, the presence of sulfate species on the surface of titania favor a high benzene yield. Cyclohexene was produced in low concentration and CO₂ was not detected in gas-phase. Enhanced photooxidative dehydrogenation activity of MoO_x/TiO₂ catalysts was attributed to the increase in surface acidity by sulfate species, which enhances hydrocarbon adsorption coverage on the catalyst surface.

On the other hand, the addition of sulfate to MoO_x/γ-Al₂O₃ catalysts was found to promote the selective mono-oxidative dehydrogenation of cyclohexane to cyclohexene [28,29]. An optimum in MoO₃ and SO₄ loadings were found to be 8 and 2.4 wt%, respectively (corresponding to MoO₃/SO₄ molar ratio equal to 2.22), while a decrease in the catalytic activity at higher sulfate loading was ascribed to MoO_x decoration by sulfates. By studying the influence of the preparation method and molybdenum loading on sulfated MoO_x/γ-Al₂O₃, it was shown that selectivity to benzene increases with increasing catalyst acidity, as the latter favors cyclohexene adsorption and thus its conversion to benzene. Close proximity of surface sulfates to octahedral polymolybdate appears to be a key parameter promoting photoactivity of these catalysts [28].

While much has been learned from the previous work, an *in situ* study of photocatalyst surfaces under UV irradiation is nevertheless needed to gain a better understanding of the surface phenomena. Typical problems of molybdenum based catalysts that need to be addressed include the role of sulfate and the deactivation occurring during gas-phase photocatalytic oxidative dehydrogenation of cyclohexane. Thus, in this study we present the results of gas phase cyclohexane photocatalytic oxidative dehydrogenation on MoO_x/TiO₂ through the analysis of products present in gas-phase exit of the reactor, complemented by *in situ* DRIFTS analysis, to monitor the photocatalyst surface in the absence and during UV irradiation.

2. Results and Discussion

2.1. Catalysts Characterization

The list of catalysts investigated and their characterization results are reported in Table 1.

Table 1. List of catalysts and their characterization results.

Catalyst	MoO ₃ ^a loading, wt%	SO ₄ ^b , wt%	SSA, m ² /g	Mo=O stretching (Raman) ^c , cm ⁻¹
DT05	0	0.6	67	-
4.7MoDT0.5	4.6	0.6	68	956
DT2	0	2.3	71	-
2MoDT2	1.8	2.2	71	953
8MoDT2	7.6	2.2	63	978

^a evaluated by ICP-MS; ^b evaluated by TG-MS analysis; ^c these results are obtained from previous studies [21,25,26].

Raman results of all the samples were reported in previous works [21,25,26]. In summary, Raman bands related to Mo-species can be observed in the range 820–1000 cm^{-1} . For all Mo-based catalysts, bands at 956 cm^{-1} on 4.7Mo/DT05, at 953 cm^{-1} on 2MoDT2, at 978 cm^{-1} on 8MoDT2 and at 956 cm^{-1} on 8Mo2S are observed and assigned to terminal Mo=O stretching of octahedral MoO_x species [30]. The increasing of wavenumber was an indication of a higher polymerization degree of Mo species at increasing loadings, corresponding to a Mo-nuclearity likely ranging from 7 to 12 [21].

2.2. Adsorption Measurement in the Absence of UV Irradiation

2.2.1. DRIFTS Analysis

Cyclohexane was admitted in absence of UV irradiation on the catalysts 2MoDT2, 4.7MoDT05, DT2 and DT05, and in Figure 1 the spectra after 1 h in presence of gas mix 2 are reported. The cyclohexane peak at 1450 cm^{-1} appears to be present on the overall tested photocatalysts, indicating the occurring of the adsorption of the hydrocarbon. This first finding was coherently with the occurring of Langmuir–Hinshelwood mechanism [23]. Together with the cyclohexane adsorption, a carbonyl vibration ($\sim 1681 \text{ cm}^{-1}$) starts to grow while an organo-sulfur vibration, found at $\sim 1354 \text{ cm}^{-1}$, decreases [31]. The decrease in the organo-sulfur vibration is more evident for the support with higher sulfate amount (DT2). These results suggest that in the absence of irradiation sulfate species initiate a redox reaction through hydrogen abstraction of cyclohexane and formation of sulfate (IV) species. In previous studies, it was concluded that reduction of the sulfate (IV) species via hydrogen abstraction may produce gas phase SO_2 and thereby loss of surface sulfur species [27].

The extent of carbonyl vibration may be related to the content of either molybdenum or sulfate, increasing in the combination of both sulfate and molybdenum. Simultaneously, an isosbestic point on the bridging-OH TiO_2 vibration, probably related to the displacement of water molecules by cyclohexane molecules, can be observed in the range 3600–3750 cm^{-1} . Surface sulfates could be highly hydrated showing a weak absorption at 1635 cm^{-1} and a strong broad absorption ranging from 3000 to 3500 cm^{-1} [32]. However, these signals are not visible because the main phenomenon is the appearance of an organo-sulfur compound (found at $\sim 1354 \text{ cm}^{-1}$) resulting from a surface reaction between sulfate and adsorbed cyclohexane that may have determined the loss of hydroxyls bonded with sulfate.

Figure 2 shows in more detail the behavior of 2MoDT2 catalyst surface during dark adsorption of gas mix 2. While the cyclohexane peak at 1450 cm^{-1} stabilizes in a few minutes, the signals at 1681 and 1354 cm^{-1} grow steadily in adsorption time, indicating a continuous surface modification. Though the peaks evolve at the same time, their behavior is not completely parallel, which indicates different surface phenomena. The 1354 cm^{-1} peak could originate from the oxidation of an organic molecule coupled to the sulfate. Other sulfate related vibrations could not be followed.

Figure 3 shows the spectra after 1 h of gas mix 3 (with H_2O in the feed) during dark adsorption on 2MoDT2, 4.7MoDT05, DT2 and Hombikat. Once again, there is an increased carbonyl vibration and a decreasing in organo-sulfur vibration. In the carbonyl area, only a single peak occurred when H_2O was absent in the gas feed (Figure 1), while when H_2O is present (Figure 3) a different product may be formed leading to 2 different vibrations in this area.

Figure 1. DRIFT spectra after 1 h of dark adsorption for gas mix 2 on DT05, DT2, 2MoDT2 and 4.7MoDT05 catalysts. Cyclohexane spectrum is shown as reference.

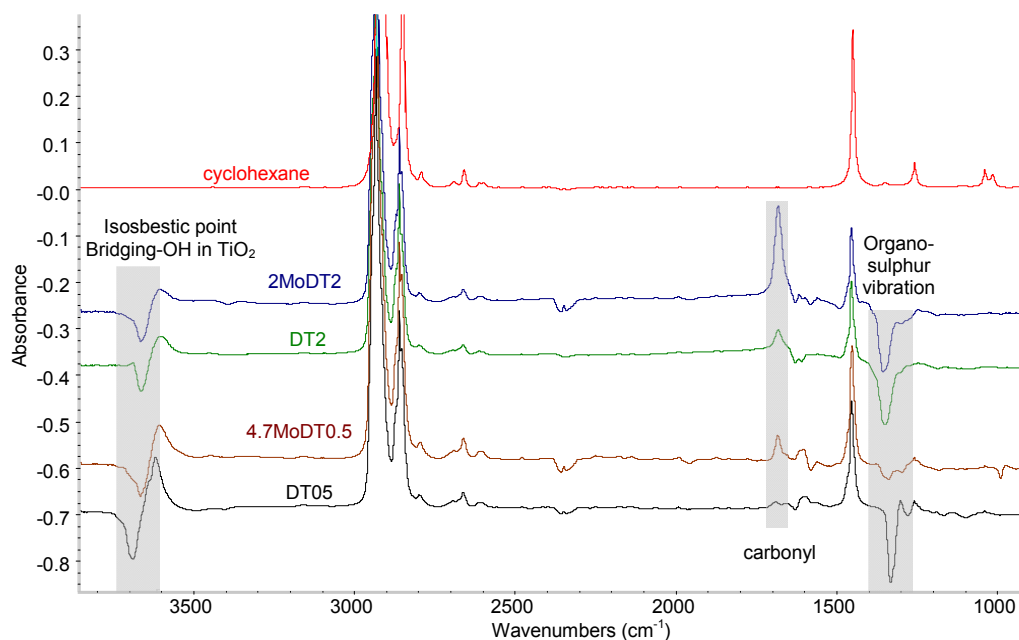
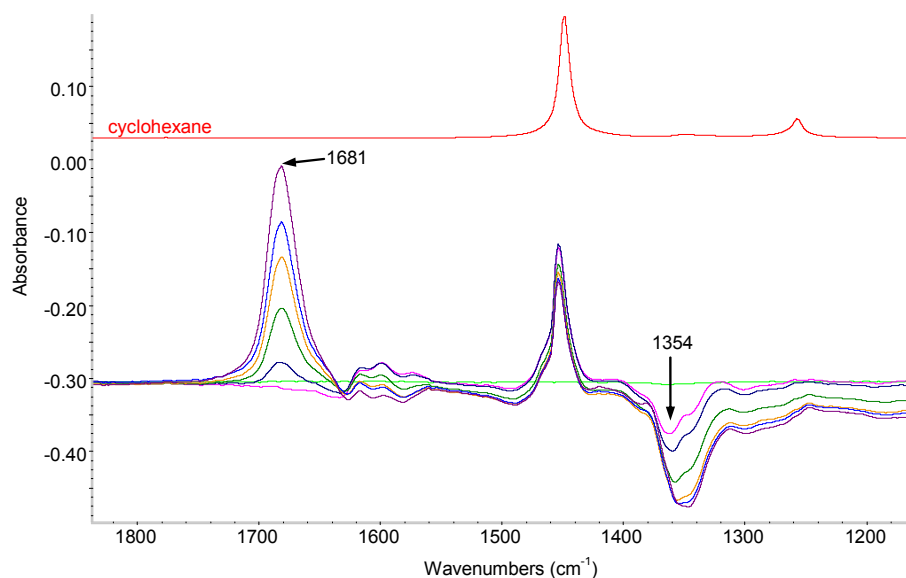


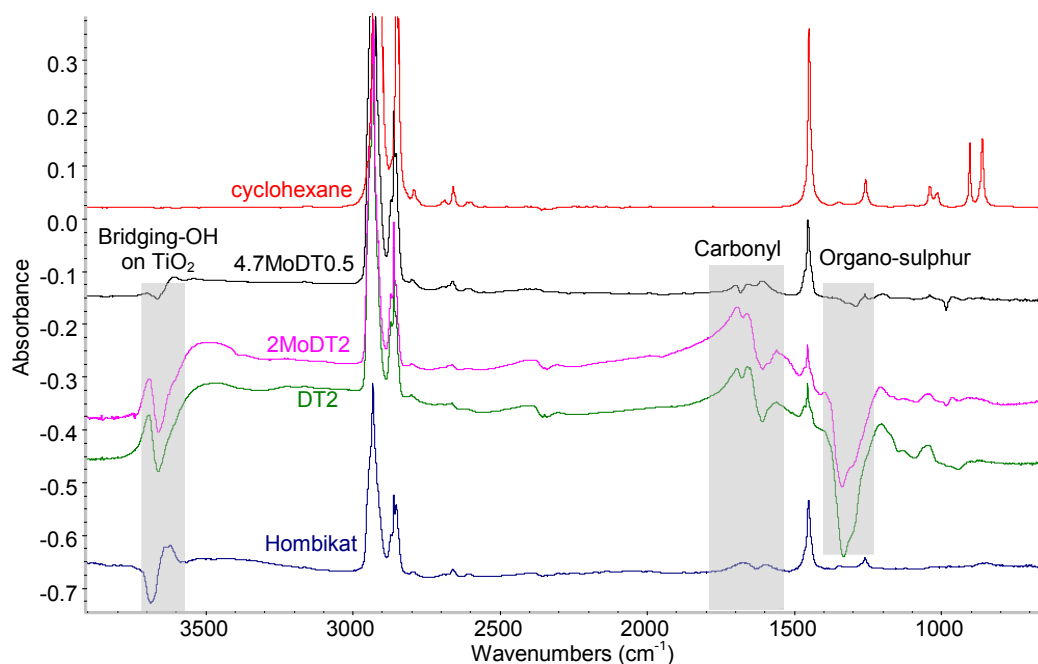
Figure 2. DRIFT spectra during 1 h of dark adsorption for gas mix 2 on 2MoDT2 catalyst.



In addition, adsorbed water may be playing a role since it absorbs around 1630 cm^{-1} and an isosbestic point may occur. To verify that the negative peak ($\sim 1354\text{ cm}^{-1}$) was related to sulfate, an unsulfated anatase- TiO_2 (Hombikat) was used as reference. The latter sample showed similar band of adsorbed cyclohexane at 1450 cm^{-1} , weak bands of carbonyl compounds with an intensity similar to that one present on the sample with low sulfate coverage (4.7MoDT05), and different hydroxyl bands. In particular, in the presence of adsorbed cyclohexane, the hydroxyl band at 3680 cm^{-1} is negative, that is hindered by cyclohexane adsorption. The hydroxyls band at 3640 cm^{-1} is instead still present, while organo-sulfur (1350 cm^{-1}) peak is not detectable. When organo-sulfur compounds are present, the band of hydroxyls at 3640 cm^{-1} is negative for the samples at high sulfate content. In the absence of

sulfate, on the Hombikat catalyst, the band of hydroxyls at 3680 cm^{-1} , instead, is negative. For this reason, the isosbestic point on the bridging-OH vibration is related to the displacement of water molecules by cyclohexane molecules, preferably interacting with hydroxyls close to the sulfate, or with OH of titania in the absence of sulfate.

Figure 3. DRIFT spectra after 1 h of dark adsorption for gas mix 3 on DT2, 2MoDT2, 4.7MoDT05 and Hombikat catalysts. Cyclohexane spectrum is shown as reference.



2.2.2. Gas Phase Analysis in the Absence of UV Irradiation

At the run starting time, the gaseous feeding stream was passed through the reactor in the absence of UV irradiation at room temperature. Adsorption of cyclohexane was observed by the decrease in its concentration. Cyclohexane breakthrough time was about 10 min. Thereafter cyclohexane outlet concentration slowly increased to reach the inlet value after about 50 min, indicating that adsorption equilibrium of cyclohexane on the catalyst surface was attained. During this period, no products in gas-phase were detected because they remained adsorbed on catalyst surface (as observed from DRIFT analysis).

A support to the formation of organo-sulfur compounds in dark conditions observed by DRIFTS could be found in our paper [24] where the amount of cyclohexane adsorbed in the dark on $\text{MoO}_x/\text{TiO}_2$ catalysts was linearly correlated with sulfate surface density. The linear increase in the amount of the cyclohexane adsorbed in dark conditions has been determined to increase cyclohexane reaction rate in presence of UV irradiation [24]. In the same paper, it was also indicated that the adsorption of cyclohexane is correlated to the corresponding increase of catalyst acidity. These results suggest that surface sulfate facilitates hydrogen abstraction from adsorbed cyclohexane, increasing its storage on catalyst surface.

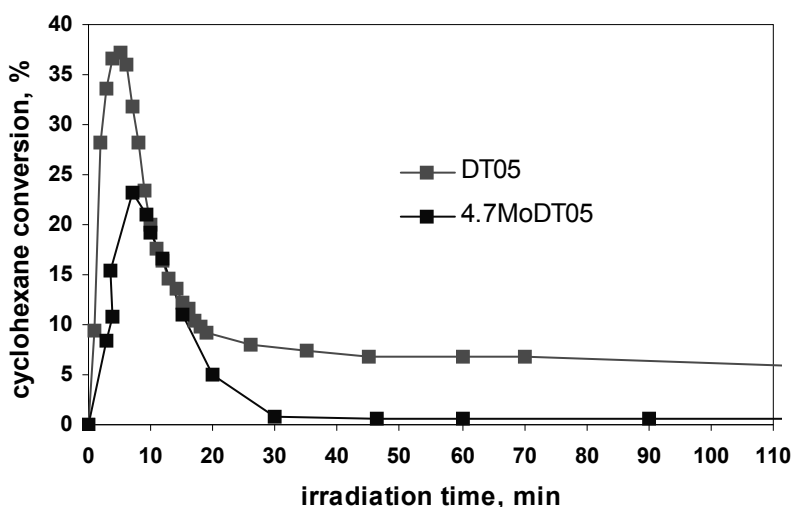
2.3. Photocatalytic Activity Tests

2.3.1. Gas Phase Analysis

Photocatalytic tests performed on titania based photocatalysts at low sulfate coverage are reported in Figure 4. Cyclohexane conversion on DT05 and 4.7MoDT05 reached a maximum after about 8 min of irradiation time and then decreased. The strong catalyst deactivation is particularly evident after this time of irradiation.

On DT05, carbon dioxide was the only product detected in gas phase (Figure 5). It started to be formed progressively; after that, the UV light was activated. In this case total carbon mass balance was closed to about 100%. In presence of Mo species, on 4.7MoDT05, the main product was benzene, whose maximum into the production was very delayed with respect both the maximum of cyclohexane conversion, and the achieving of cyclohexane conversion steady state conditions. In fact, the maximum outlet concentration of benzene was 7 ppm after 55 min. CO₂ concentration showed a steady state formation value of 10 ppm. Cyclohexene was formed before benzene in agreement with the mechanism reported in [21], that considered consecutive steps of oxidative dehydrogenation going through cyclohexene, as intermediate, to get finally benzene.

Figure 4. Cyclohexane conversion on DT05 and 4.7MoDT05 during UV irradiation.



The comparison of cyclohexane conversion over DT2, 2MoDT2 and 8MoDT2 is shown in Figure 6. A maximum value was reached after about 5 min on all catalysts, then activity decreased approaching a steady state conversion. On 2MoDT2, maximum cyclohexane conversion was about 45%, decreasing to about 10% in 90 min. With the same sulfate content, increasing Mo loading up to 8 wt% MoO₃, the initial maximum conversion was lower, about 15%, while steady state conversion was 2.3% after 30 min. Therefore, the progressive coverage of the titania surface by MoO_x species resulted in a decreased initial and steady state cyclohexane conversions according to our previous results [21]. On DT2 the initial maximum conversion was higher with respect to 8MoDT2 (about 25%), while steady state conversion was similar. Thus, with lower sulfate coverage, steady state photocatalyst activity was smaller, so underlining the relevance of sulfate presence on the photocatalysts performances.

Figure 5. (a) Benzene outlet concentration; (b) carbon dioxide outlet concentration and (c) cyclohexene outlet concentration on DT05 and 4.7MoDT05 catalysts during UV irradiation.

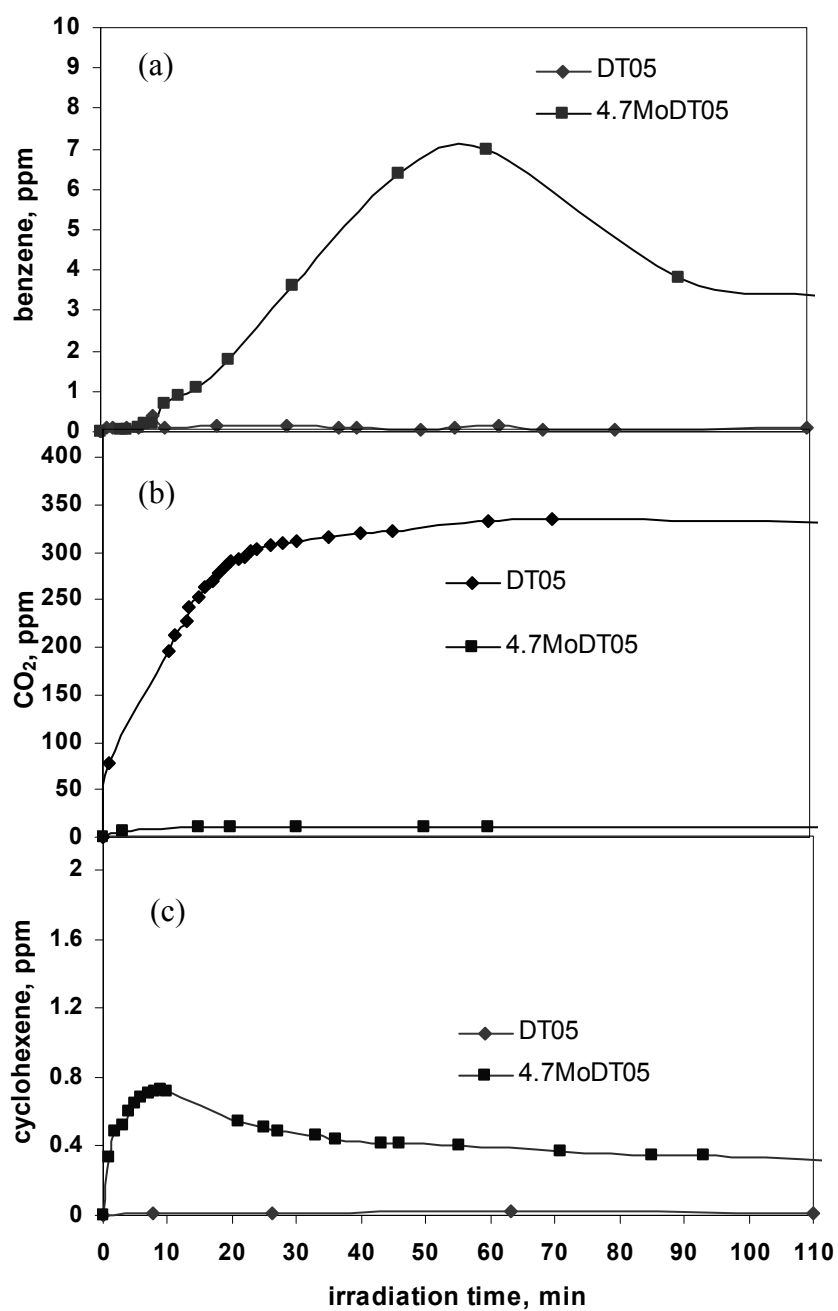


Figure 6. Cyclohexane conversion on DT2, 2MoDT2 and 8MoDT2 catalysts during UV irradiation.

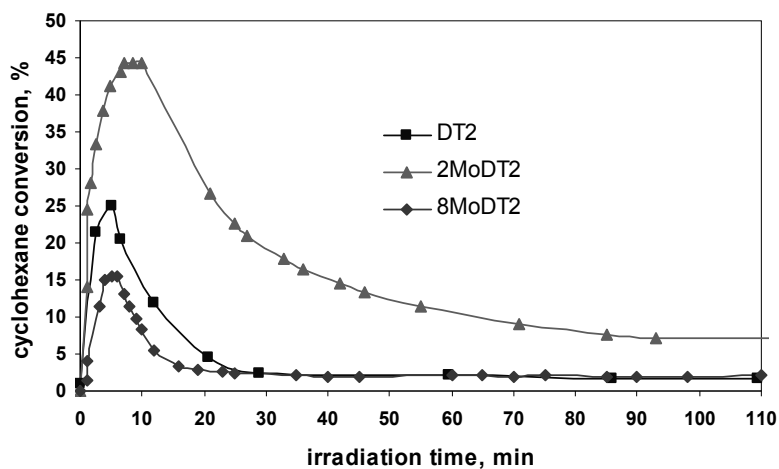
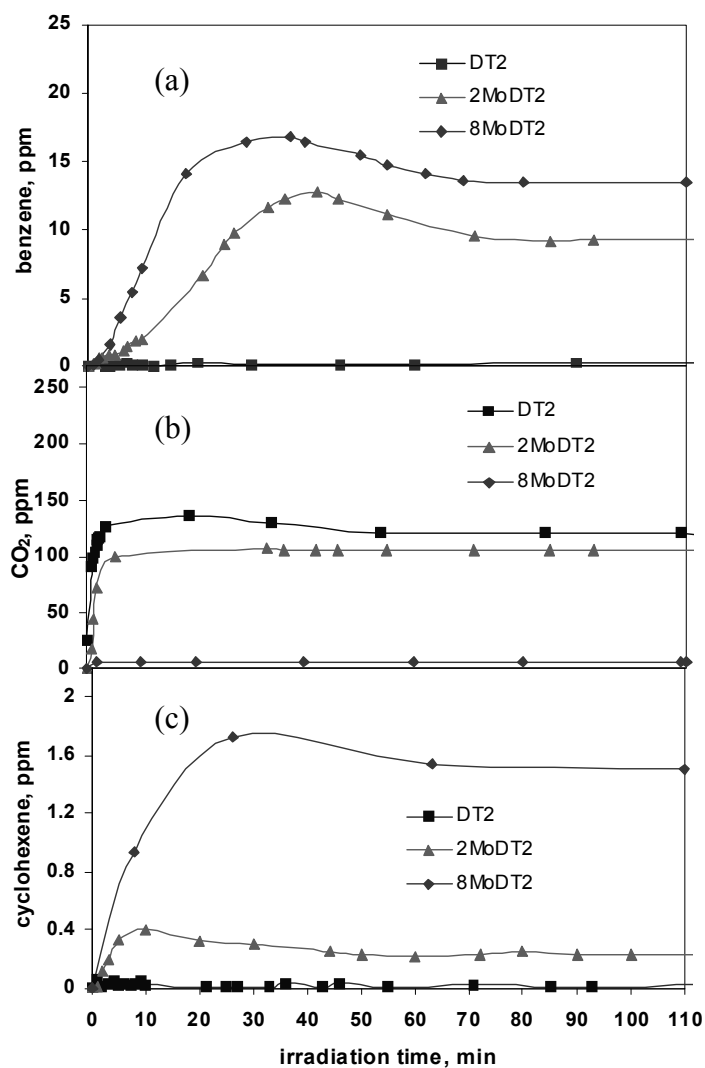


Figure 7. (a) Benzene outlet concentration, (b) carbon dioxide outlet concentration and (c) cyclohexene outlet concentration on DT2, 2MoDT2 and 8MoDT2 catalysts during UV irradiation.



On all MoO_x/TiO₂ catalysts, reaction products were benzene, CO₂ and few amount of cyclohexene (Figure 7). Benzene concentration showed a maximum (17 ppm after 36 min on 8MoDT2 and 13 ppm after 45 min on 2MoDT2), while CO₂ concentration was 100 ppm on 2MoDT2 and 6 ppm on 8MoDT2. As observed for DT05 catalysts, the only product observed on DT2 was carbon dioxide and its concentration was the highest.

The higher cyclohexene concentration was recorded for 8MoDT2 whereas its formation was negligible on 2MoDT2, reaching a value less than 1 ppm.

In summary, gas phase analysis of cyclohexane and reaction products evidenced that the presence of MoO_x species on the surface of titania, at same sulfate content, changes the selectivity of the catalyst with increasing molybdenum loading. These results indicate that the interaction between titania and supported molybdenum oxide plays an essential role in the catalyst selectivity. In addition also the amount of surface sulfate influenced benzene yield, decreasing when the sulfate content is lower.

2.3.2. DRIFTS Analysis

The results of photocatalytic reaction are shown in Figure 8a,b for gas mix 2. The CH stretching vibration of cyclohexane increases steadily during illumination probably because cyclohexane adsorption was still occurring, possibly as the result of light induced dehydration of the surface, making free new adsorption sites. So besides dehydration and the continued adsorption of cyclohexane on TiO₂ sites, also depletion of hydroxyl groups occurs during photoreaction, as showed by the increasing negative absorption in the range 3200–3800 cm⁻¹. This has been also observed performing the reaction in liquid phase.

During UV irradiation, the peaks, likely to be ascribed to adsorbed cyclohexanone (1691 and 1671 cm⁻¹) were found (Figure 4a), indicating the occurrence of an oxidation step in the reaction. The formation of two different peaks could be related to the presence of different active sites at the surface, but also to a different ketone. The peak at 1671 cm⁻¹, in liquid phase cyclohexane photooxidation, was attributed to a stronger adsorption site, while the 1691 cm⁻¹ to a weaker cyclohexanone adsorption site [19]. The position of these peaks is, however, different from the one observed during cyclohexanone dark adsorption (1681cm⁻¹), so during this step, the formation of different surface products could be supposed. An examination of the literature was then performed with the aim to support the latter hypothesis.

In a paper concerning the cyclohexene photo-oxidation over V/TiO₂ catalysts [33], cyclohexenone was formed during irradiation. One of the most intense band of this unsaturated carbonyl compound is located at 1692 cm⁻¹. So the signal at 1691 cm⁻¹ could be ascribed also to the presence of cyclohexenone, in turn formed from cyclohexene [33]. In addition, it should be considered that C=C stretching frequency of alkenes lies in the range between 1680–1620 cm⁻¹ [34], therefore it overlaps to the signals due to adsorbed ketones. The formation of cyclohexene was also found in cyclohexane oxidation at low temperatures using copper chloride in pyridine as catalyst [35] and by liquid phase photocatalytic oxidation of cyclohexane on TiO₂ in various solvents [15]. In particular, by using dichloromethane as solvent, the presence of cyclohexene and cyclohexenone was found. Thus it is not possible to exclude the formation of an unsaturated cyclic hydrocarbon in the presence of molybdenum, taking into account also that the cyclohexene adsorbs on the surface through the C=C double bond, and the contribution of the -HC=CH- stretching would therefore be absent [36].

With regard to benzene detected in gas phase, it is not observed in DRIFTS analysis, in agreement with the low affinity evinced in [21] for the titania surface. Both the two kind of hydroxyls disappear during the photoreaction.

Figure 8. DRIFT spectra during 90 min of UV irradiation for gas mix 2 on 2MoDT2 catalyst in the range 1100–1925 cm^{-1} (a) and in the range 2750–3900 cm^{-1} (b).

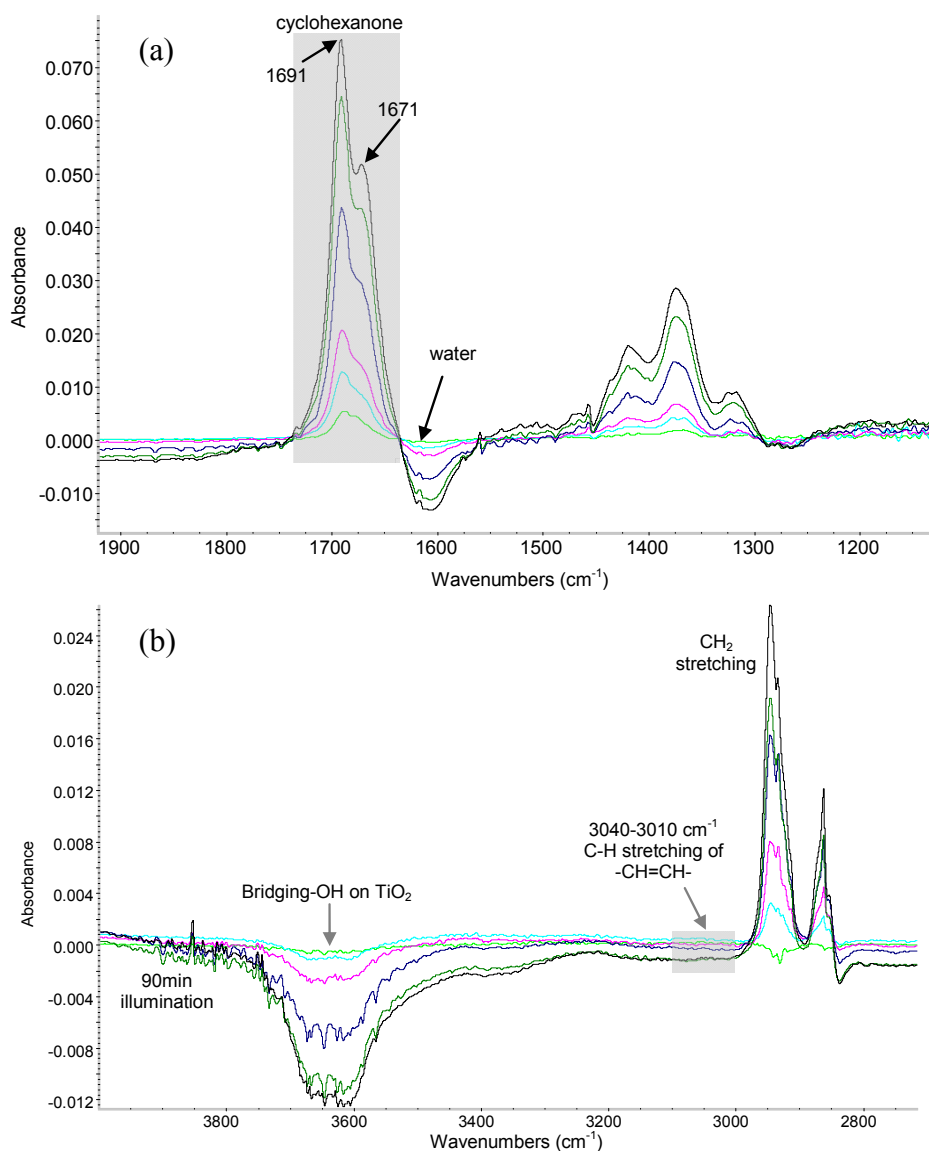
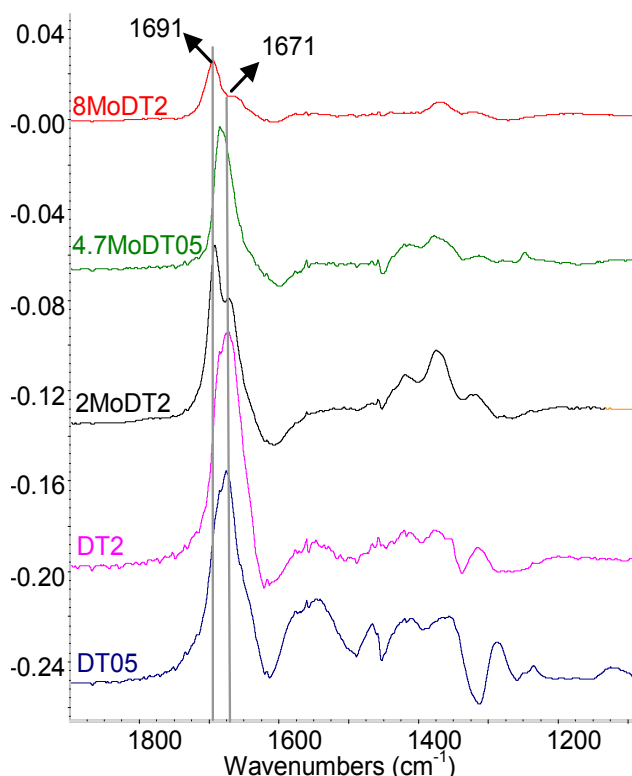


Figure 9 compares the photocatalytic activity of 8MoDT2, 4.7MoDT05 and 2MoDT2 with DT2 and DT05 supports. The DT05 and DT2 supports show similar carbonyl absorptions, with stronger 1671 cm^{-1} vibration. When molybdenum is added to the catalyst, a decrease in this peak is observed and the 1691 cm^{-1} peak becomes more prominent. Similar to 2MoDT2, 8MoDT2 photocatalyst shows two bands at 1671 and 1691 cm^{-1} . The latter signal could be ascribed also in this case to cyclohexenone. The contribution at about 1690 cm^{-1} is not visible for DT2 and DT05, indicating that the formation of this compound is due probably correlated to the presence of molybdenum. The band at 1690 cm^{-1} is also not present on 4.7MoDT05. This result could be explained considering that gas phase results on 4.7MoDT05 (Figures 4 and 5) showed the lowest activity and benzene production

with together a strong deactivation during UV irradiation. Therefore, in this case, the formation of carbonylic compounds is predominant. On the other hand, the formation of oxygenated products (stronger 1671 cm^{-1} vibration) is observed for all catalysts, and a decrease in the formation of these products occurs with increasing molybdenum loading confirmed by the decrease of the band at 1671 cm^{-1} when molybdenum is added on TiO_2 surface.

Figure 9. DRIFT spectra after 90 min of UV irradiation for gas mix 2 on 8MoDT2, 4.7MoDT05, 2MoDT2, DT2 and DT05 catalysts.

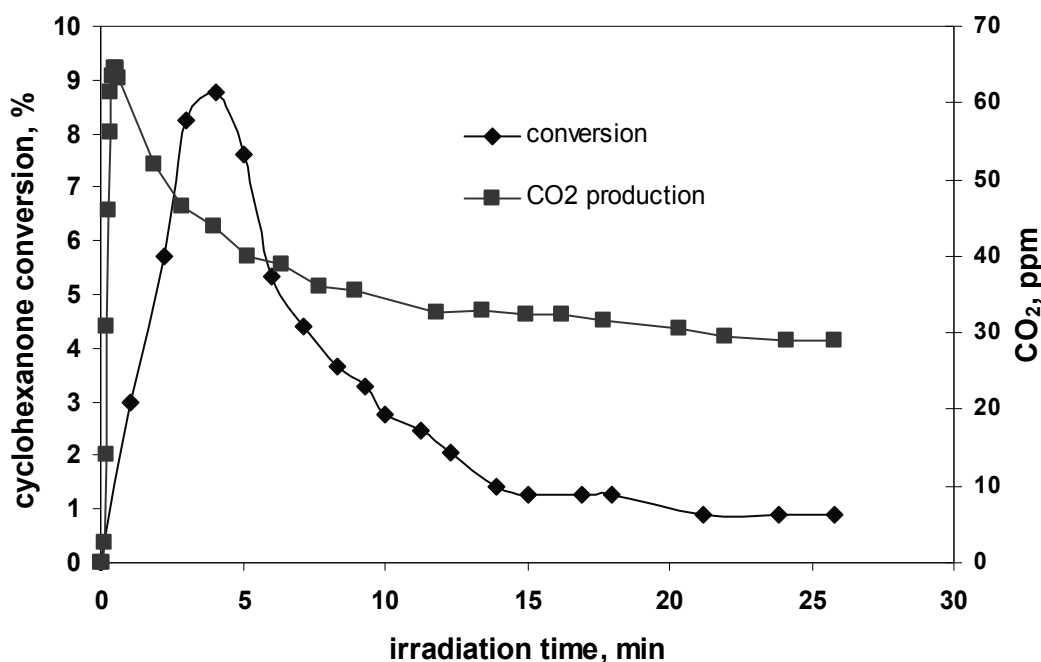


The other data to consider are the bands in the region from 1300 cm^{-1} to about 1450 cm^{-1} , ascribed to the carbon deposits on the catalyst surface during the photoreaction, which determine the deactivation of catalyst observed in the literature [37]. These observations suggest that these species are formed on bare titania, where total oxidation occurs preferentially, while Mo-species hinder titania surface sites active for total oxidation. The photocatalytic tests performed on all catalysts revealed that a rapid decays of activity occurred in the first minutes on stream (Figures 4 and 6). This initial decrease of activity is probably due to a poisoning of the surface by carbon deposits, blocking of a part of the catalytic surface sites.

2.4. Further Test to Assess Intermediates

With the aim to confirm if carbonylic compounds are the responsible of catalyst deactivation, a photocatalytic test on 8MoDT2 was carried out by feeding cyclohexanone with the same operating conditions used for cyclohexane.

The obtained results are reported in Figure 10.

Figure 10. Cyclohexanone conversion and CO₂ concentration during UV irradiation.

Maximum cyclohexanone conversion was about 9%, and then activity decreased to 1% in 15 min. A steady state condition was obtained after about 21 min of irradiation with a conversion of approximately 0.9%. Carbon dioxide was formed immediately after the UV sources were switched on and reached a concentration of about 60 ppm after an irradiation time of 0.5 min. CO₂ was the only observed product and no other reaction products were detected in gas phase. These results evidenced that cyclohexanone (carbonyl compounds shown by DRIFTS spectra) is the precursor for CO₂ production. According to DRIFTS spectra, the accumulation on surface of intermediates formed by cyclohexanone oxidation during irradiation is the responsible of catalyst deactivation.

With regard to the influence of sulfate, a considerable decrease in the formation of carboxylates is observed with higher molybdenum and sulfate content confirming that the simultaneous presence of Mo-species and sulfate sharply increases photocatalytic activity and selectivity. The acidity induced by the sulfate on TiO₂ surface [38] furnishes hydrocarbon activation towards partial oxidation and supplying the initial step in the absence of irradiation [24]. However, if the sulfate is lost during dark adsorption, it can induce a deactivation of catalyst under illumination.

For gas mix 3, when H₂O is also present, almost no reaction has been observed for the molybdenum catalysts. The decrease in reactivity due to the hydration of metal oxides has been discussed in literature [39].

An example is shown in Figure 11, for the 4.7MoDT05 catalysts, in which very small peaks were observed under UV irradiation. The increase of CH stretching vibration indicates that cyclohexane adsorption on the catalyst surface is still occurring evidencing a deactivation phenomenon. The contribution of the reaction products to the spectra is very low, only visible by the formation of small peaks between 1800–1000 cm⁻¹ and the decrease of the TiO₂ bridging-OH.

Figure 11. DRIFT spectra during 90 min of UV irradiation for gas mix 3 on 4.7MoDT05 catalyst.

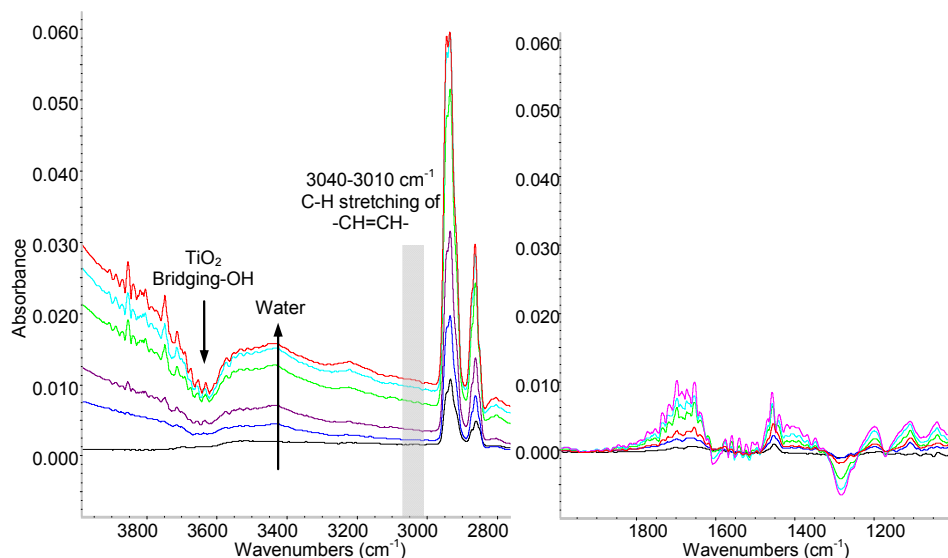
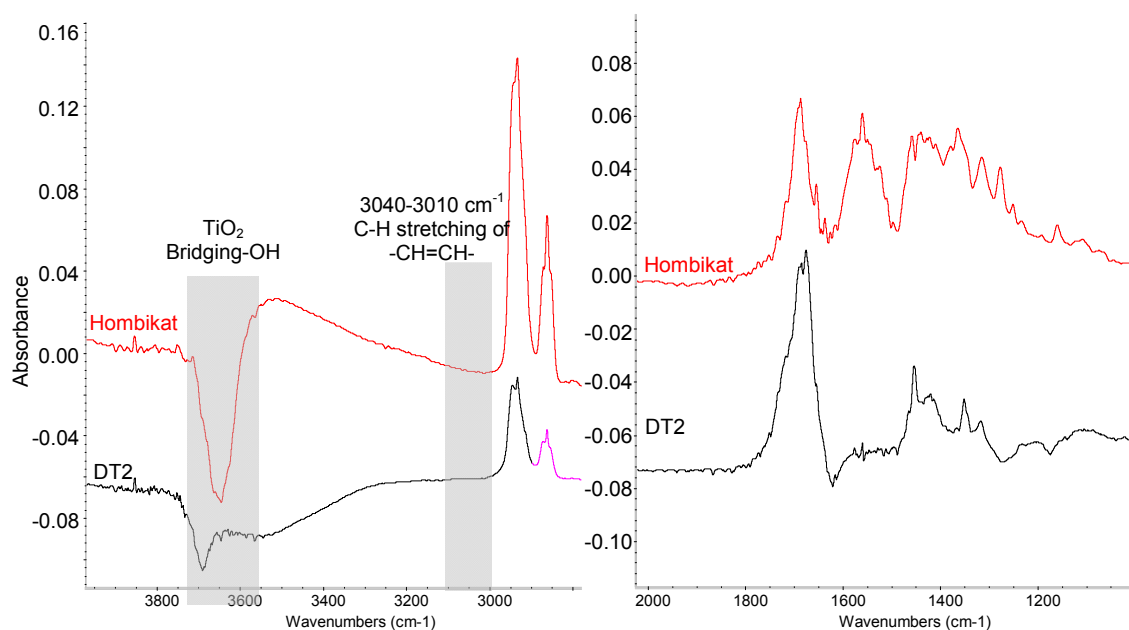


Figure 12. DRIFT spectra after 90 min of UV irradiation for gas mix 3 on DT2 and Hombikat catalysts.



Under gas mix 3 flow better results were observed when there was no molybdenum on the TiO_2 surface, as can be seen in Figure 12. While on $\text{MoO}_x/\text{TiO}_2$ catalysts, the water presence in the gas feed greatly decreased the product formation, in DT2 this effect was not observed. The reactivity of DT2 under gas mix 2 (without H_2O) and 3 (with H_2O) showed similar reaction products and spectral intensity. As expected from previous work, no peaks related to unsaturated hydrocarbons formation were observed on DT2 [21]. Hombikat is also shown as reference, which appears to catalyze the formation of more surface products and higher bridging-OH deactivation than the ones observed for sulfated TiO_2 . This last result is a further confirmation of the role of sulfate in the deactivation of photocatalysts.

3. Experimental Section

3.1. Catalysts Preparation and Characterization

Two titanias were used as supports: two commercial titania samples (DT and DT51 by Millenium Inorganic Chemicals) with different sulfate content (respectively 0.5 wt% and 2 wt% expressed as SO_3) contributed from the experimental procedure used for the synthesis of samples [40]. The samples are named, respectively, DT2 and DT05 with reference to the sulfate content. MoO_x -based catalysts were prepared by wet impregnation of titania with aqueous solution of ammonium heptamolybdate ($(\text{NH}_4)_6\text{Mo}_7\text{O}_{24} \cdot 4\text{H}_2\text{O}$), followed by drying at 120 °C and calcination at 400 °C for 3 h. Unsulfated titania (Hombikat) was used as reference.

Thermogravimetric analysis (TG-DSC-MS) was carried out in air flow on powder samples with a thermoanalyzer (Q600, TA) in the range 20–1000 °C with an heating rate of 10 °C/min. Sulfate content has been evaluated from the weight loss in the range in which the release of SO_2 occurred. Specific surface area was obtained by N_2 adsorption-desorption isotherm at –196 °C with a Costech Sorptometer 1040. Powder samples were treated at 150 °C for 2 h in He flow (99.9990%) before testing. Laser Raman spectra of powder samples were obtained with a Dispersive MicroRaman (Invia, Renishaw), equipped with 785 nm diode-laser, in the range 100–2500 cm^{-1} Raman shift. Chemical analysis of molybdenum loading was performed by inductive coupled plasma-mass spectrometry (7500c ICP-MS, Agilent) after microwave digestion (Ethos Plus from Milestone) of samples in HNO_3/HCl and HF/HCl mixtures.

3.2. Gas phase Analysis

Photocatalytic tests were carried out feeding 1000 ppm cyclohexane, 1500 ppm oxygen and 1600 ppm water in N_2 (total flow rate: 830 (stp) cm^3/min) to a continuous gas-solid annular photocatalytic fixed-bed reactor. The tests were carried out in presence of water in order to minimize catalyst deactivation as reported in literature [37].

Oxygen and nitrogen were fed from cylinders, nitrogen being the carrier gas for cyclohexane and water vaporized from two temperature controlled saturators containing pure cyclohexane and water. The gas flow rates were measured and controlled by mass flow controllers (Brooks Instrument). The annular section of the reactor [27] (reactor volume: 7 l) was realized with two axially mounted 500 mm long quartz tubes of 140 and 40 mm diameter, respectively. The reactor was equipped with seven 40 W UV fluorescent lamps providing photons wavelengths in the range from 300 to 425 nm, with primary peak centered at 365 nm. One lamp (UVA Cleo Performance 40 W, Philips) was centered inside the inner tube while the others (R-UVA TLK 40 W/10R flood lamp, Philips) were located symmetrically around the reactor.

Although light sources vary in their intensity, they have the same emission spectrum and in the case of photocatalytic oxidative dehydrogenation of cyclohexane, the selectivity of the reaction was not influenced by light intensity [23].

The overall system composed of UV lamps and photoreactor are covered by aluminum foils to minimize the dispersion of the photons in the space surrounding the photoreactor. In order to avoid temperature gradients in the reactor caused by irradiation, the temperature was controlled to 35 ± 2 °C

by cooling fans. The catalytic reactor bed was prepared *in situ*, by coating quartz flakes previously loaded in the annular section of a quartz continuous flow reactor with aqueous slurry of catalysts powder. The coated flakes were dried at 120 °C for 24 h in order to remove the excess of physisorbed water. This treatment resulted in uniform coating well adhering to the quartz flakes surface. The gas composition was continuously determined by on line analyzers connected to a PC for data acquisition. CO and CO₂ concentration is measured by an on line non dispersive IR analyzer (Uras 10, Hartmann & Braun), working on the basis of specific adsorption of IR radiation (wavelength from 2 to 8 μm). Oxygen, cyclohexane and reaction products composition is determined by an on line quadrupole mass detector (MD800, ThermoFinnigan) that can analyze the outlet reactor gas, introduced into a heated silica capillary, up to $m/z = 800$.

3.3. DRIFTS Analysis

A layer of KBr powder was introduced in the DRIFTS (3 window cell) holder [41], over which each of the different catalysts and supports were deposited and pressed. The catalysts were heated up to 120 °C for 30 min in He flow (app. 30mL/min) to remove weakly adsorbed water from the surface.

Different gas mixtures (100mL/min flow) were prepared for the catalytic tests:

Gas mix 1: 1000ppm Cyclohexane, 1500ppm O₂

Gas mix 2: 1000ppm Cyclohexane, 5000ppm O₂

Gas mix 3: 1000 ppm Cyclohexane, 250 ppm H₂O, 5000ppm O₂

Further, for DRIFTS analysis, nitrogen is the carrier gas for cyclohexane and water vaporized from two temperature controlled saturators containing pure cyclohexane and water.

A background (128 scan averages) of the dried catalyst at room temperature was taken and used for the adsorption step, which was followed with IR during 40–60 min, until surface stabilization was achieved. A spectrum (128 scan averages) was taken after adsorption stabilization, which was used as background for the reaction step. Reaction was continued for 90 min; the first minute of collection was performed in the dark, and the rest was done under irradiation by a 150 W Xe light with a light diffuser. All spectra, except for background spectra, consisted of 64 averaged scans and water vapor correction has been applied to most of them.

Only the background spectrum was collected at room temperature, while during the irradiation the temperature increased up to a value very similar to that one of the fixed bed reactor used for gas phase analysis. In this way, the selectivity of the reaction was not different.

4. Conclusions

From coupling of gas phase and DRIFTS analysis, a deeper knowledge of phenomena occurring during photocatalytic selective oxidation of cyclohexane on MoO_x/TiO₂ was obtained.

During adsorption measurements in the absence of UV irradiation, there is a clear indication of organo-sulfur compound formation accompanied by H-abstraction by the acidic sulfate species. The accompanying stepwise reduction of the sulfate by protons causes formation of SO₂ and thereby loss of surface sulfur. The decrease in surface sulfur during the dark adsorption experiment leads to a subsequent initial decrease in photocatalytic activity during irradiation since the acidity induced by the sulfate facilitates hydrocarbon activation in partial oxidation of cyclohexane after supplying the initial

step in the absence of irradiation. The further decrease of photoactivity during irradiation is due to a poisoning of the surface by carbonaceous species derived from carbonylic compounds formed on bare titania, blocking of a portion of the catalytic surface sites. A considerable decrease in the rate of poisoning by carbonaceous species is observed at higher molybdenum and sulfate contents, confirming that the simultaneous presence of Mo-species and sulfate enhances photocatalytic activity and selectivity. Gas phase analysis of cyclohexane and reaction products evidenced that the presence of MoO_x species at same sulfate coverage increases the selectivity of the catalyst with increasing molybdenum content indicating that the interaction between titania and supported molybdenum oxide plays an essential role in changing the catalyst selectivity. In addition increasing coverage of surface sulfate influenced benzene yield.

Conflicts of Interest

No author of the present manuscript has a direct financial relation with the commercial identities mentioned in the paper that might lead to a conflict of interest.

References

1. Sannino, D.; Vaiano, V.; Sacco, O.; Ciambelli, P. Mathematical modelling of photocatalytic degradation of methylene blue under visible light irradiation. *J. Environ. Chem. Eng.* **2013**, *1*, 56–60.
2. Sacco, O.; Stoller, M.; Vaiano, V.; Ciambelli, P.; Chianese, A.; Sannino, D. Photocatalytic Degradation of Organic Dyes under Visible Light on N-Doped TiO₂ Photocatalysts. *Int. J. Photoenergy* **2012**, Article ID 626759:1–Article ID 626759:8.
3. Murcia, J.J.; Hidalgo, M.C.; Navío, J.A.; Vaiano, V.; Sannino, D.; Ciambelli, P. Cyclohexane photocatalytic oxidation on Pt/TiO₂ catalysts. *Catal. Today* **2013**, *209*, 164–169.
4. Stoller, M.; Movassaghi, K.; Chianese, A. Photocatalytic degradation of orange II in aqueous solutions by immobilized nanostructured titanium dioxide. *Chem. Eng. Trans.* **2011**, *24*, 229–234.
5. Ibrahim, H.; de Lasa, H. Photo-catalytic conversion of air borne pollutants: Effect of catalyst type and catalyst loading in a novel photo-CREC-air unit. *Appl. Catal. B* **2002**, *38*, 201–213.
6. Augugliaro, V.; Bellardita, M.; Loddo, V.; Palmisano, G.; Palmisano, L.; Yurdakal, S. Overview on oxidation mechanisms of organic compounds by TiO₂ in heterogeneous photocatalysis. *J. Photochem. Photobiol. C* **2012**, *13*, 224–245.
7. Sannino, D.; Vaiano, V.; Isupova, L.A.; Ciambelli, P. Heterogeneous Photo-Fenton Oxidation of Organic Pollutants on Structured Catalysts. *J. Adv. Oxid. Technol.* **2012**, *15*, 294–300.
8. Sannino, D.; Vaiano, V.; Ciambelli, P.; Isupova, L.A. Structured catalysts for photo-Fenton oxidation of acetic acid. *Catal. Today* **2011**, *161*, 255–259.
9. Molinari, A.; Amadelli, R.; Mazzacani, A.; Sartori, G.; Maldotti, A. Tetraalkylammonium and sodium decatungstate heterogenized on silica: Effects of the nature of cations on the photocatalytic oxidation of organic substrates. *Langmuir* **2002**, *18*, 5400–5405.
10. Maldotti, A.; Molinari, A.; Amadelli, R. Photocatalysis with organized systems for the oxofunctionalization of hydrocarbons by O₂. *Chem. Rev.* **2002**, *102*, 3811–3836.

11. Li, X.; Chen, G.; Po-Lock, Y.; Kotal, C. Photocatalytic oxidation of cyclohexane over TiO₂ nanoparticles by molecular oxygen under mild conditions. *J. Chem. Technol. Biotechnol.* **2003**, *78*, 1246–1251.
12. Stoller, M.; Miranda, L.; Chianese, A. Optimal Feed location in a Spinning Disc Reactor for the Production of TiO₂ Nanoparticles. *Chem. Eng. Trans.* **2009**; *17*, 993–998.
13. de Caprariis, B.; Di Rita, M.; Stoller, M.; Verdone, N.; Chianese, A. Reaction-precipitation by a spinning disc reactor: Influence of hydrodynamics on nanoparticles production. *Chem. Eng. Sci.* **2012**, *76*, 73–78.
14. Boarini, P.; Carassiti, V.; Maldotti, A.; Amadelli, R. Photocatalytic oxygenation of cyclohexane on titanium dioxide suspensions: Effect of the solvent and of oxygen. *Langmuir* **1998**, *14*, 2080–2085.
15. Almquist, C.B.; Biswas, P. The photo-oxidation of cyclohexane on titanium dioxide: an investigation of competitive adsorption and its effects on product formation and selectivity. *Appl. Catal. A* **2001**, *214*, 259–271.
16. Berg, O.; Hamdy, M.S.; Maschmeyer, T.; Moulijn, J.A.; Bonn, M.; Mul, G. On the wavelength-dependent performance of Cr-doped silica in selective photo-oxidation. *J. Phys. Chem. C* **2008**, *112*, 5471–5475.
17. Maldotti, A.; Amadelli, R.; Varani, G.; Tollari, S.; Porta, F. Photocatalytic processes with polyoxotungstates: Oxidation of cyclohexylamine. *Inorg. Chem.* **1994**, *33*, 2968–2973.
18. Teramura, K.; Tanaka, T.; Yamamoto, T.; Funabiki, T. Photo-oxidation of cyclohexane over alumina-supported vanadium oxide catalyst. *J. Mol. Catal. A* **2001**, *165*, 299–301.
19. Almeida, A.R.; Moulijn, J.A.; Mul, G. *In situ* ATR-FTIR study on the selective photo-oxidation of cyclohexane over anatase TiO₂. *J. Phys. Chem. C* **2008**, *112*, 1552–1561.
20. Xu, W.; Raftery, D.; Francisco, J.S. Effect of irradiation sources and oxygen concentration on the photocatalytic oxidation of 2-propanol and acetone studied by *in situ* FTIR. *J. Phys. Chem. B* **2003**, *107*, 4537–4544.
21. Ciambelli, P.; Sannino, D.; Palma, V.; Vaiano, V.; Bickley, R.I. Reaction mechanism of cyclohexane selective photo-oxidation to benzene on molybdena/titania catalysts. *Appl. Catal. A* **2008**, *349*, 140–147.
22. Ciambelli, P.; Sannino, D.; Palma, V.; Vaiano, V.; Mazzei, R.S. Improved Performances of a Fluidized Bed Photoreactor by a Microscale Illumination System. *Int. J. Photoenergy* **2009**, Article ID 709365:1– Article ID 709365:7.
23. Palma, V.; Sannino, D.; Vaiano, V.; Ciambelli, P. Fluidized-Bed Reactor for the Intensification of Gas-Phase Photocatalytic Oxidative Dehydrogenation of Cyclohexane. *Ind. Eng. Chem. Res.* **2010**, *49*, 10279–10286.
24. Ciambelli, P.; Sannino, D.; Palma, V.; Vaiano, V. The effect of sulfate doping on nanosized TiO₂ and MoO_x/TiO₂ catalysts in cyclohexane photooxidative dehydrogenation. *Int. J. Photoenergy* **2008**, Article ID 258631:1–Article ID 258631:8.
25. Ciambelli, P.; Sannino, D.; Palma, V.; Vaiano, V. Photocatalysed selective oxidation of cyclohexane to benzene on MoO_x/TiO₂. *Catal. Today* **2005**, *99*, 143–149.
26. Ciambelli, P.; Sannino, D.; Palma, V.; Vaiano, V. Cyclohexane photocatalytic oxidative dehydrogenation to benzene on sulfated titania supported MoO_x. *Stud. Surf. Sci. Catal.* **2005**, *155*, 179–187.

27. Sannino, D.; Vaiano, V.; Ciambelli, P.; Eloy, P.; Gaigneaux, E.M. Avoiding the deactivation of sulfated MoO_x/TiO₂ catalysts in the photocatalytic cyclohexane oxidative dehydrogenation by a fluidized bed photoreactor. *Appl. Catal. A* **2011**, *394*, 71–78.
28. Ciambelli, P.; Sannino, D.; Palma, V.; Vaiano, V.; Eloy, P.; Dury, F.; Gaigneaux, E.M. Tuning the selectivity of MoO_x supported catalysts for cyclohexane photo oxidehydrogenation. *Catal. Today* **2007**, *128*, 251–257.
29. Ciambelli, P.; Sannino, D.; Palma, V.; Vaiano, V.; Mazzei, R.S.; Eloy, P.; Gaigneaux, E.M. Photocatalytic cyclohexane oxidehydrogenation on sulfated MoO_x/gamma-Al₂O₃ catalysts. *Catal. Today* **2009**, *141*, 367–373.
30. Cheng, C.P.; Schrader, G.L. Characterization of supported molybdate catalysts during preparation using laser Raman spectroscopy. *J. Catal.* **1979**, *60*, 276–294.
31. Bellamy, L.J.; Mayo, D.W. Infrared frequency effects of lone pair interactions with antibonding orbitals on adjacent atoms. *J. Phys. Chem.* **1976**, *80*, 1217–1220.
32. Bezrodna, T.; Puchkovska, G.; Shimanovska, V.; Chashechnikova, I.; Khalyavka, T.; Baran, J. Pyridine-TiO₂ surface interaction as a probe for surface active centers analysis. *Appl. Surface Sci.* **2003**, *214*, 222–231.
33. Mul, G.; Wasylenko, W.; Hamdy, M.S.; Frei, H. Cyclohexene photo-oxidation over vanadia catalyst analyzed by time resolved ATR-FT-IR spectroscopy. *Phys. Chem. Chem. Phys.* **2008**, *10*, 3131–3137.
34. Coates, J. Vibrational spectroscopy: Instrumentation for infrared and Raman spectroscopy. *Appl. Spectrosc. Rev.* **1998**, *33*, 267–425.
35. Schuchardt, U.; Pereira, R.; Rufo, M. Iron(III) and copper(II) catalysed cyclohexane oxidation by molecular oxygen in the presence of tert-butyl hydroperoxide. *J. Mol. Catal. A* **1998**, *135*, 257–262.
36. Manner, W.L.; Girolami, G.S.; Nuzzo, R.G. Sequential dehydrogenation of unsaturated cyclic C₅ and C₅ hydrocarbons on Pt(111). *J. Phys. Chem. B* **1998**, *102*, 10295–10306.
37. Einaga, H.; Futamura, S.; Ibusuki, T. Heterogeneous photocatalytic oxidation of benzene, toluene, cyclohexene and cyclohexane in humidified air: Comparison of decomposition behavior on photoirradiated TiO₂ catalyst. *Appl. Catal. B* **2002**, *38*, 215–225.
38. Ciambelli, P.; Fortuna, M.E.; Sannino, D.; Baldacci, A. The influence of sulfate on the catalytic properties of V₂O₅-TiO₂ and WO₃-TiO₂ in the reduction of nitric oxide with ammonia. *Catal. Today* **1996**, *29*, 161–164.
39. Amano, F.; Yamaguchi, T.; Tanaka, T. Photocatalytic oxidation of propylene with molecular oxygen over highly dispersed titanium, vanadium, and chromium oxides on silica. *J. Phys. Chem. B* **2006**, *110*, 281–288.
40. Taranto, J.; Frochot, D.; Pichat, P. Photocatalytic treatment of air: Comparison of various TiO₂, coating methods, and supports using methanol or *n*-Octane as test pollutant. *Ind. Eng. Chem. Res.* **2009**, *48*, 6229–6236.

41. Carneiro, J.T.; Moulijn, J.A.; Mul, G. Photocatalytic oxidation of cyclohexane by titanium dioxide: Catalyst deactivation and regeneration. *J. Catal.* **2010**, *273*, 199–210.

© 2013 by the authors; licensee MDPI, Basel, Switzerland. This article is an open access article distributed under the terms and conditions of the Creative Commons Attribution license (<http://creativecommons.org/licenses/by/3.0/>).